

Electronic Supplementary Material (ESI)

Water adsorption behaviour of CAU-10-H: A thorough investigation of its structure-property relationships

Dominik Fröhlich^{a,b}, Evangelia Pantatosaki^c, Panagiotis D. Kolokathis^c, Karen Markey^d, Helge Reinsch^e, Max Baumgartner^a, Monique A. van der Veen^f, Dirk E. De Vos^d, Norbert Stock^e, George K. Papadopoulos^{c,g}, Stefan K. Henninger^{a,*} and Christoph Janiak^{b,*}

- a. Fraunhofer Institute for Solar Energy Systems ISE, Heidenhofstrasse 2, 79110 Freiburg, Germany; Fax: 49 761 4588913; Tel: +49 761 45882117
- b. Institut für Anorganische Chemie und Strukturchemie, Heinrich-Heine-Universität Düsseldorf, Universitätsstr. 1, 40225 Düsseldorf, Germany, Tel.: +49 211 8112286,
- c. School of Chemical Engineering, National Technical University of Athens, 9 Heron Polytechniou Street, 157 80 Athens, Greece
- d. Centre for Surface Chemistry and Catalysis, University of Leuven, Kasteelpark Arenberg 23, 3001 Leuven, Belgium
- e. Institute of Inorganic Chemistry, Christian-Albrechts-University Kiel, Max-Eyth-Str. 2, D-24118 Kiel, Germany
- f. Catalysis Engineering, Department of Chemical Engineering, Delft University of Technology, 2826 Delft, The Netherlands
- g. Institute for Medical Engineering and Science, Massachusetts Institute of Technology, Cambridge, Massachusetts 02139, USA

Emails

- 1) dominik.froehlich@ise.fraunhofer.de
- 2) evpanta@chemeng.ntua.gr
- 3) tkolokathis@yahoo.gr
- 4) Karen.Markey@biw.kuleuven.be
- 5) hreinsch@ac.uni-kiel.de
- 6) max.baumgartner@ise.fraunhofer.de
- 7) M.A.vanderVeen@tudelft.nl
- 8) dirk.devos@biw.kuleuven.be
- 9) stock@ac.uni-kiel.de
- 10) gkppap@chemeng.ntua.gr
- *11) stefan.henninger@ise.fraunhofer.de
- *12) janiak@uni-duesseldorf.de

1) Synthesis of CAU-10-H:

CAU-10-H was synthesized from 505 g (0.75 mol) of aluminium sulfate hydrate ($\text{Al}_2(\text{SO}_4)_3 \cdot 18\text{H}_2\text{O}$) dissolved in 2.5 L of H_2O , and 132 g (0.79 mol) isophthalic acid dissolved in 625 mL of DMF. The two solutions were combined in a 5 L round bottom flask. The combined mixture was heated under reflux for 117 h. After cooling down the precipitate was filtered, redispersed for washing in 3 L of H_2O by sonication and stirring. The dispersion was filtered again and dried for 4 days at 100 °C and after this activated for 2 days at 120°C in vacuum. The total yield was 150 g (91 %) CAU-10-H. Surface area $S_{\text{BET}} = 564\text{m}^2\text{g}^{-1}$ and pore volume $0.26\text{ cm}^3\text{g}^{-1}$.

2) SEM images of the coating:

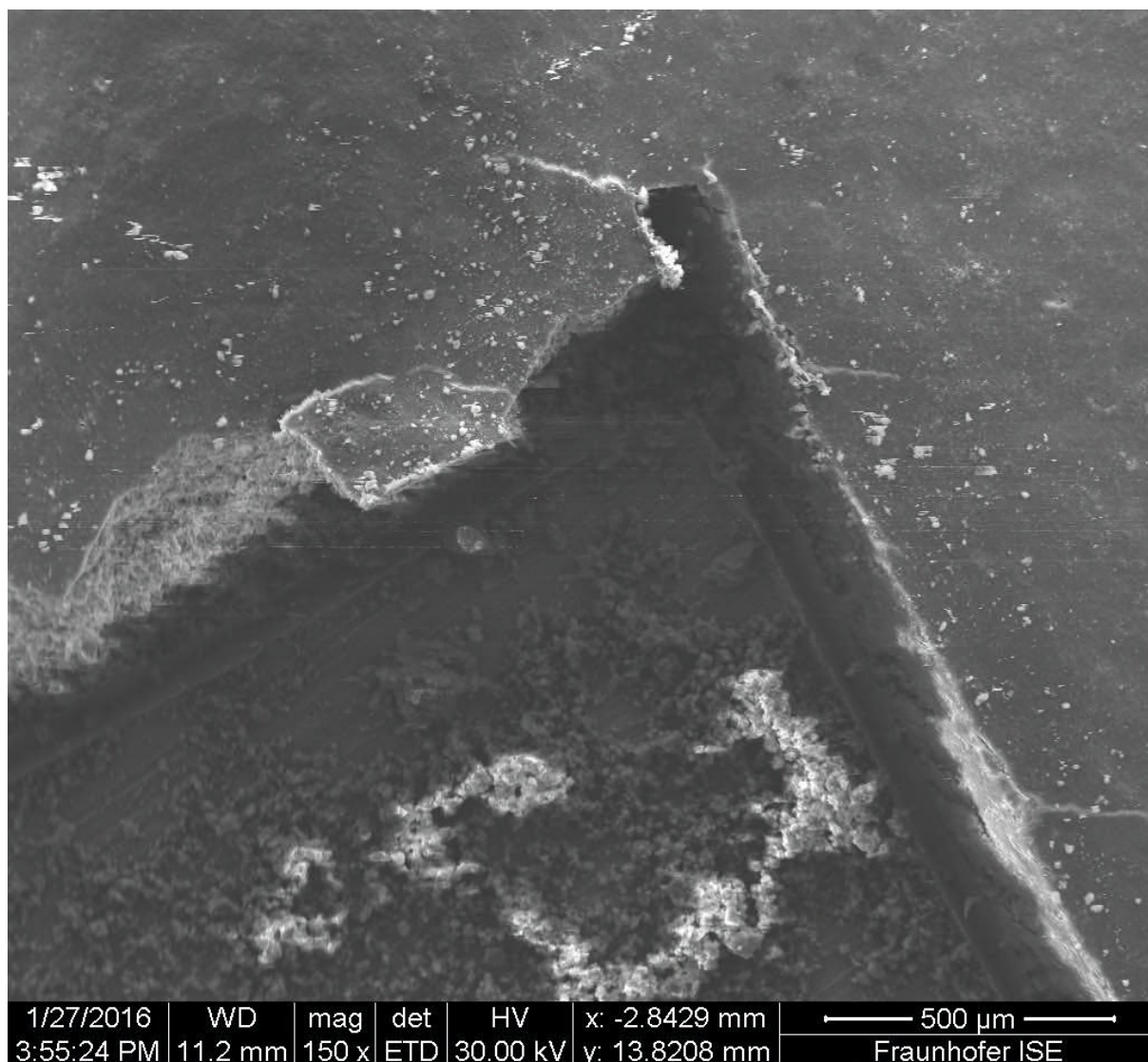


Fig. S1 SEM image of cross-section of CAU-10-H coating. Part of the coating was removed to get a better impression on the uniformity and thickness of the coating.

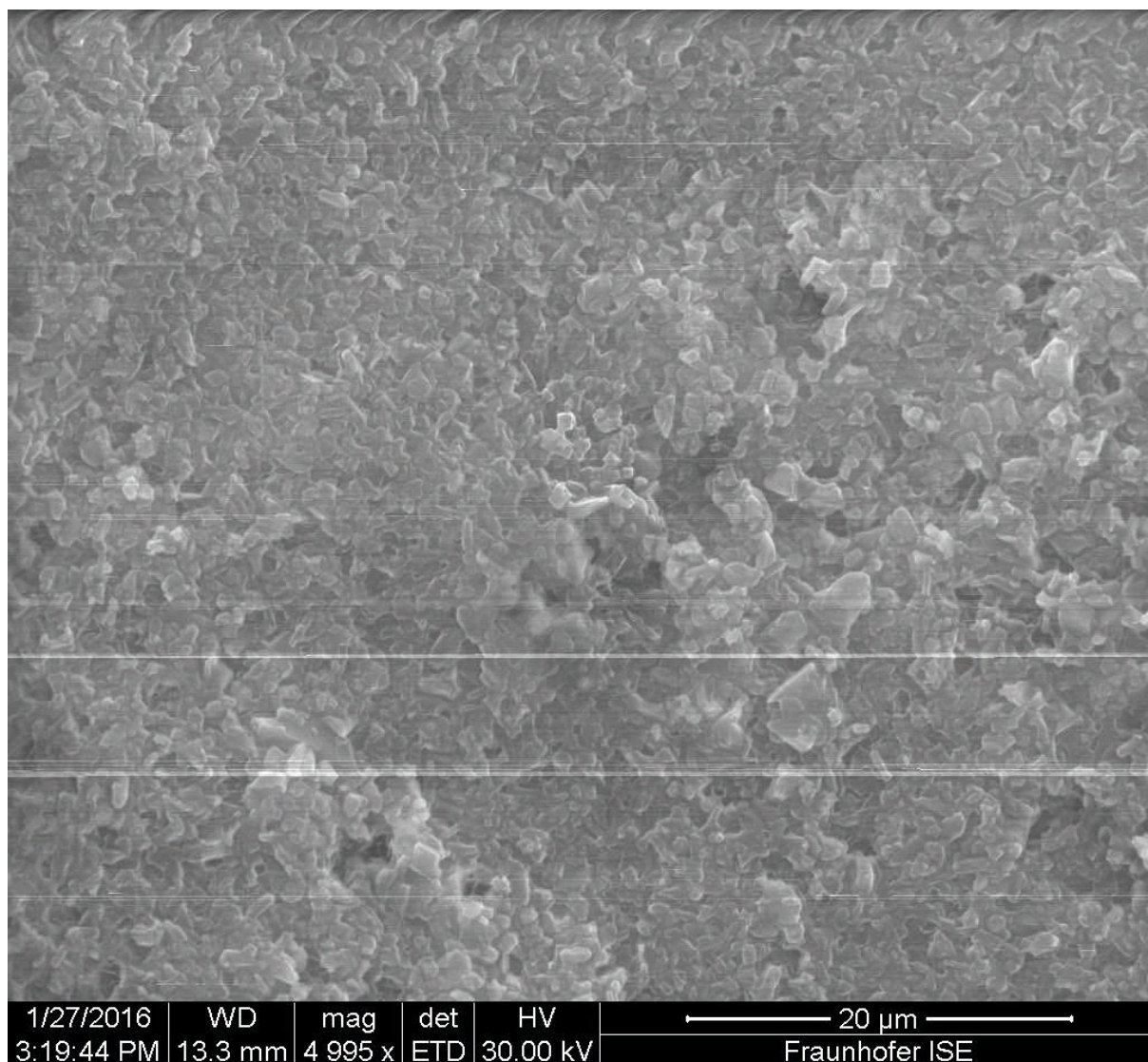


Fig. S2 SEM image of the CAU-10-H coating.

3) Experimental section for capillary PXRD measurements

The in-situ measurements at different relative humidity values unambiguously proved a phase transition between the known non-centrosymmetric form of CAU-10-H and a not yet reported dry, centrosymmetric conformation. In the light of these results, high-resolution PXRD data was analysed and crystal structures of the dry and the wet form were obtained by Rietveld refinement. The samples were loaded in capillaries and sealed either under ambient conditions after filtration (hydrated form) or after evacuation at 0.1 mbar and heating to 200 °C (dried form). The data was collected using a STOE Stadi-P diffractometer equipped with a Mythen detector using monochromated $\text{CuK}_{\alpha 1}$ radiation. The software used for indexing and refinements was TOPAS.

The extinction conditions for the dried form are in agreement with the space group $I4_1/amd$ and thus the crystal structure of the isostructural CAU-10- CH_3 was utilised as a starting model for Rietveld

refinement. The functional groups were removed from the structural model and the positions of all other atoms could be successfully refined after employing restraints.

Although the structure of hydrated CAU-10-H has been reported previously, the structure was reevaluated since better PXRD data could be obtained. Hence for the structure determination of the hydrated form the already reported crystal structure data¹ was taken as a starting model. Initially the position of the linker molecules was optimised by force-field methods using Materials Studio. This first model was used in the Rietveld refinement. Additional electron density found by Fourier Synthesis was attributed to water molecules inside the pores and subsequently their occupancy was also refined. The carbon backbones of the linker molecules were refined as rigid bodies and all other atoms were freely refined using restraints until convergence was achieved. The determination of the position of water molecules is usually very challenging using solely in-house PXRD data. For an ultimate proof, it would be advisable to measure neutron diffraction data on deuterated samples. Nevertheless, in the absence of such data the obtained position and the observed distances are in good agreement with expected values for moderate to strong hydrogen bonds. The residual electron density could be attributed to seven independent oxygen atoms representing water molecules.

The most relevant crystallographic data is summarised in Table S1 and the asymmetric units are given in Figures S3 and S4. Relevant bond distances are given in Tables S2 and S3. The final Rietveld plots are given in Figures S5 and S6.

Table S1 Final parameters of the Rietveld refinements.

CAU-10-H	Hydrated	Dry
space group	$I4_1$	$I4_1/amd$
$a = b$ [Å]	21.2928(4)	21.5214(7)
c [Å]	10.7305(3)	10.3218(4)
V [Å ³]	4865.0(2)	4780.7(3)
R_{WP} / %	6.8	4.3
R_{Bragg} / %	3.2	0.6
GoF	1.54	1.03
wavelength	Cu $K\alpha_1$	Cu $K\alpha_1$

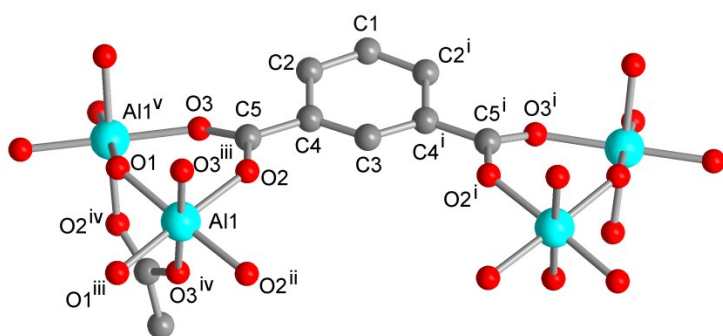


Figure S3 Extended asymmetric unit of CAU-10H-dry with full Al coordination spheres and full ligand bridging mode. Symmetry transformations i = 1-x, y, z; ii = x, -y, -z; iii = 0.25+y, 0.25-x, -0.25+z; iv = 0.25+y, -0.25+x, 0.25-z; v = 0.25-y, -0.25+x, 0.25+z; selected distances and angles are given in Table S2.

Table S2 Relevant bond distances (Å) and angles (°) for CAU-10-H-dry.^a

Al1-O1(O1 ⁱⁱⁱ)	1.855(9)	O2-C5	1.252(13)
Al1-O3 ^{iii,iv}	1.888(11)	O3-C5	1.282(13)
Al1-O2(O2 ⁱⁱ)	1.903(11)	C1-C2	1.400(11)
		C2-C4	1.405(12)
O1-Al1-O1 ⁱⁱⁱ	88.853(3)	C3-C4	1.384(12)
O1-Al1-O3 ⁱⁱⁱ	88.2(3)	C4-C5	1.471(11)
O1-Al1-O3 ^{iv}	91.0(3)		
O1-Al1-O2	92.3(3)		
O1-Al1-O2 ⁱⁱ	178.0(3)		
O3 ⁱⁱⁱ -Al1-O3 ^{iv}	178.9(5)		
O3 ⁱⁱⁱ -Al1-O2	90.7(4)		
O3 ⁱⁱⁱ -Al1-O2 ⁱⁱ	90.1(4)		
O2-Al1-O2 ⁱⁱ	86.5(4)		
Al1-O1-Al1 ^v	126.657(4)		

^a Symmetry transformations: ii = x, -y, -z; iii = 0.25+y, 0.25-x, -0.25+z; iv = 0.25+y, -0.25+x, 0.25-z; v = 0.25-y, -0.25+x, 0.25+z

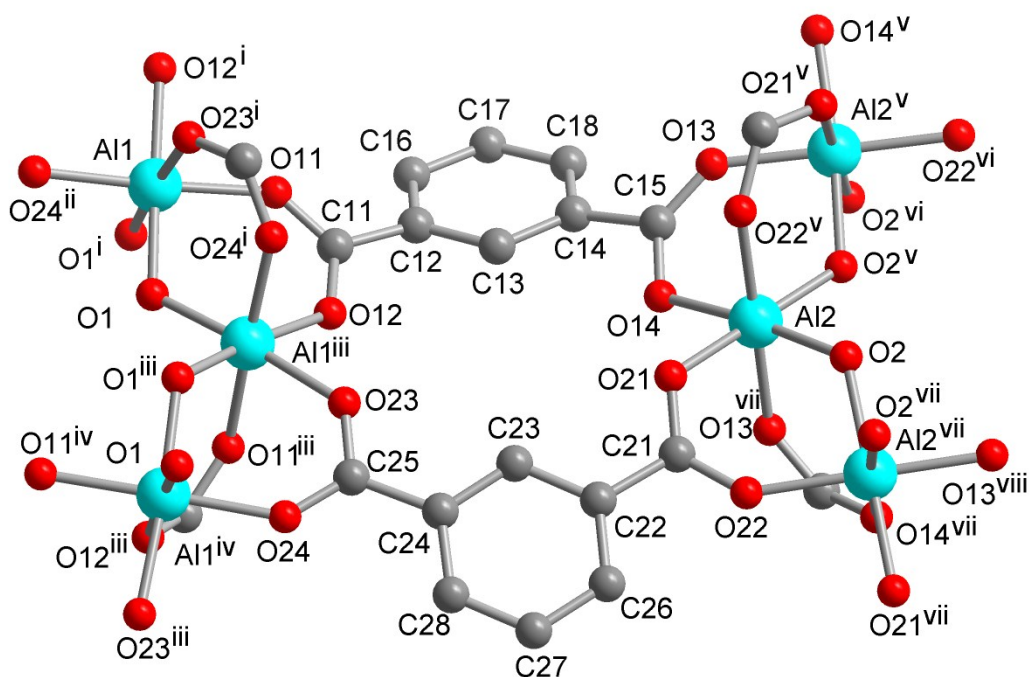


Figure S4 Extended asymmetric unit of CAU-10H-H₂O with full Al coordination spheres and full ligand bridging mode. Symmetry transformations i = 0.5–y, x, –0.25+z; ii = 0.5–x, 0.5–y, –0.5+z; iii = y, 0.5–x, 0.25+z; iv = 0.5–x, 0.5–y, 0.5+z; v = 0.5+y, 1–x, –0.25+z; vi = 1.5–x, 0.5–y, –0.5+z; vii = 1–y, –0.5+x, 0.25+z; viii = 1.5–x, 0.5–y, 0.5+z; selected distances and angles are given in Table S3. Crystal water guest molecules are not shown.

Table S3 Relevant bond distances (Å) and angles (°) for CAU-10-H-H₂O including potential hydrogen bonds. Distances within the rigid bodies were not refined and therefore are given without standard uncertainties.^a

Al1-O1	1.871(16)	C14-C15	1.467
Al1-O1 ⁱ	1.875(15)	C16-C17	1.393
Al1-O24 ⁱⁱ	1.897(10)	C17-C18	1.393
Al1-O12 ⁱ	1.903(12)	O13-C15	1.237(7)
Al1-O11	1.906(10)	O14-C15	1.236(9)
Al1-O23 ⁱ	1.967(12)		
O11-C11	1.238(9)	Al2-O13 ^{vii}	1.890(11)
O12-C11	1.264(9)	Al2-O2 ^v	1.906(14)
C11-C12	1.467	Al2-O22 ^v	1.920(11)
C12-C13	1.401	Al2-O21	1.921(13)
C12-C16	1.415	Al2-O2 ^{iv}	1.923(15)
C13-C14	1.401	Al2-O14	1.964(12)
C14-C18	1.415	O21 C21	1.221(8)

O22	C21	1.300(8)
C21	C22	1.479
C22	C23	1.408
C22	C26	1.415
C23	C24	1.408
C24	C28	1.415
C24	C25	1.479
C26	C27	1.392
C27	C28	1.392
O23	C25	1.283(9)
O24	C25	1.239(9)
O1-Al1-O1 ⁱ		92.2(6)
O1-Al1-O24 ⁱⁱ		89.2(6)
O1-Al1-O12 ⁱ		173.3(7)
O1-Al1-O11		94.2(6)
O1-Al1-O23 ⁱ		86.6 (5)
O1 ⁱ -Al1-O24 ⁱⁱ		92.2 (6)
O1 ⁱ -Al1-O12 ⁱ		94.6(5)
O1 ⁱ -Al1-O11		87.6 (5)
O1 ⁱ -Al1-O23 ⁱ		175.7 (6)
O24 ⁱⁱ -Al1-O12 ⁱ		90.4(6)
O24 ⁱⁱ -Al1-O11		176.6 (5)
O24 ⁱⁱ -Al1-O23 ⁱ		91.8 (6)
O12 ⁱ -Al1-O11		86.2 (5)
O12 ⁱ -Al1-O23 ⁱ		86.7(5)
O11-Al1-O23 ⁱ		88.4(5)
O13 ^{vii} -Al2-O2 ^v		92.1 (5)
O13 ^{vii} -Al2-O22 ^v		179.2(6)
O13 ^{vii} -Al2-O21		88.2(4)
O13 ^{vii} -Al2-O2		88.1(5)
O13 ^{vii} -Al2-O14		87.5(5)
O2 ^v -Al2-O22 ^v		87.9(5)
O2 ^v -Al2-O21		179.1(6)

O2 ^v -Al2-O2	89.6(6)
O2 ^v -Al2-O14	93.2(5)
O22 ^v -Al2-O21	91.8(4)
O22 ^v -Al2-O2	92.7(5)
O22 ^v -Al2-O14	91.7(5)
O21-Al2-O2	89.6(5)
O21-Al2-O14	87.6 (5)
O2-Al2-O14	174.9(6)

Potential hydrogen bonds (Å):

Og1-Og2	2.728(23)
Og1-O1	2.944(18)
Og2-Og3	2.766(21)
Og2-Og7	3.052(50)
Og2-Og3	3.145(25)
Og3-Og7	3.018(46)
Og3-Og4	3.084(24)
Og4-O2	2.798(20)
Og4-O21	2.954(20)
Og4-O2	3.095(21)
Og5-O12	2.879(19)
Og5-Og6	3.016(22)
Og5-Og7	3.068(26)
Og5-O23	3.129(21)
Og6-Og7	2.727(54)
Og6-Og6	2.894(18)

Symmetry transformations

i = 0.5−y, x, −0.25+z; ii = 0.5−x, 0.5−y, −0.5+z; iii = y, 0.5−x, 0.25+z; iv = 0.5−x, 0.5−y, 0.5+z; v = 0.5+y, 1−x, −0.25+z; vi = 1.5−x, 0.5−y, −0.5+z; vii = 1−y, −0.5+x, 0.25+z; viii = 1.5−x, 0.5−y, 0.5+z.

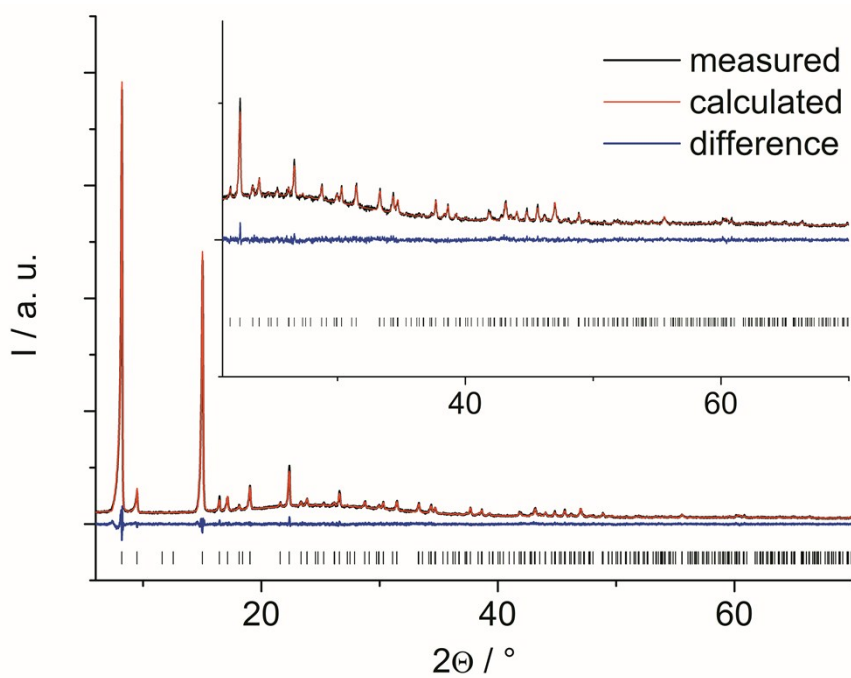


Figure S5 Final Rietveld Plot for CAU-10-H-dry. The black line is the experimental data, the red line gives the calculated fit, the blue line is the difference curve. Vertical bars mark the Bragg reflection positions.

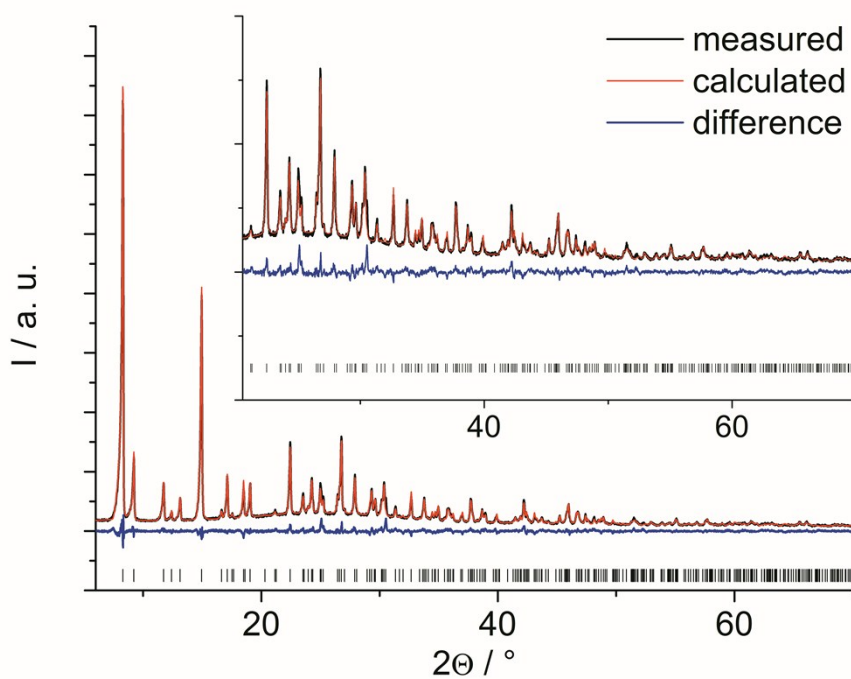


Figure S6 Final Rietveld Plot for CAU-10-H-H₂O. The black line is the experimental data, the red line gives the calculated fit, the blue line is the difference curve. Vertical bars mark the Bragg reflection positions.

Crystallographic Information Files (CIFs):

data_

_chemical_name_mineral **CAU10dry**

_cell_length_a 21.52137(72)

_cell_length_b 21.52137(72)

_cell_length_c 10.32179(44)

_cell_angle_alpha 90

_cell_angle_beta 90

_cell_angle_gamma 90

_cell_volume 4780.74(38)

_symmetry_space_group_name_H-M I41/amdz

loop_

_symmetry_equiv_pos_as_xyz

'-x, -y, -z'

'-x, y, z'

'-x+1/2, -y, z+1/2'

'-x+1/2, y, -z+1/2'

'-y+1/4, -x+1/4, -z-1/4'

'-y+1/4, x-1/4, z+1/4'

'-y-1/4, -x+1/4, z-1/4'

'-y-1/4, x-1/4, -z+1/4'

'y+1/4, -x+1/4, z-1/4'

'y+1/4, x-1/4, -z+1/4'

'y-1/4, -x+1/4, -z-1/4'

'y-1/4, x-1/4, z+1/4'

'x, -y, -z'

'x, y, z'

'x+1/2, -y, z+1/2'

'x+1/2, y, -z+1/2'

'-x+1/2, -y+1/2, -z+1/2'

'-x+1/2, y+1/2, z+1/2'

'-x, -y+1/2, z'

'-x, y+1/2, -z'

'-y-1/4, -x-1/4, -z+1/4'

'-y-1/4, x+1/4, z-1/4'

'-y+1/4, -x-1/4, z+1/4'

'-y+1/4, x+1/4, -z-1/4'

'y-1/4, -x-1/4, z+1/4'

'y-1/4, x+1/4, -z-1/4'

'y+1/4, -x-1/4, -z+1/4'

'y+1/4, x+1/4, z-1/4'

'x+1/2, -y+1/2, -z+1/2'

'x+1/2, y+1/2, z+1/2'

'x, -y+1/2, z'

'x, y+1/2, -z'

```

loop_
_atom_site_label
_atom_site_type_symbol
_atom_site_symmetry_multiplicity
_atom_site_fract_x
_atom_site_fract_y
_atom_site_fract_z
_atom_site_occupancy
_atom_site_B_iso_or_equiv
Al1 Al 16 0.31840(42) 0 0 1 0.74(12)
O1 O 16 0.25684(37) 0.00684(37) 0.125 1 0.74(12)
O2 O 32 0.38279(48) 0.00937(40) 0.12478(72) 1 0.74(12)
O3 O 32 0.33677(37) 0.06753(49) 0.27693(79) 1 0.74(12)
C1 C 32 0.5 0.08862(93) 0.4789(17) 1 0.74(12)
C2 C 32 0.44355(22) 0.07462(54) 0.41817(74) 1 0.74(12)
C3 C 32 0.5 0.0373(10) 0.2334(18) 1 0.74(12)
C4 C 16 0.44385(28) 0.05337(55) 0.28952(74) 1 0.74(12)
C5 C 16 0.38363(36) 0.03863(56) 0.22955(87) 1 0.74(12)

```

```

data_
_chemical_name_mineral CAU10H2O
_cell_length_a 21.29280(42)
_cell_length_b 21.29280(42)
_cell_length_c 10.73045(29)
_cell_angle_alpha 90
_cell_angle_beta 90
_cell_angle_gamma 90
_cell_volume 4865.01(23)
_symmetry_space_group_name_H-M I41

```

```

loop_
_symmetry_equiv_pos_as_xyz
'-x+1/2, -y+1/2, z+1/2'
'-y, x+1/2, z+1/4'
'y+1/2, -x, z-1/4'
'x, y, z'
'-x, -y, z'
'-y+1/2, x, z-1/4'
'y, -x+1/2, z+1/4'
'x+1/2, y+1/2, z+1/2'

```

```

loop_
_atom_site_label
_atom_site_type_symbol
_atom_site_symmetry_multiplicity
_atom_site_fract_x

```

_atom_site_fract_y

_atom_site_fract_z

_atom_site_occupancy

_atom_site_B_iso_or_equiv

Al1 Al 8 0.25543(34) 0.31384(35) 0.24427(82) 1 1.04(11)
Al2 Al 8 0.68023(32) 0.24569(33) 0.49332(85) 1 1.04(11)
O1 O 8 0.24869(46) 0.25942(44) 0.3805(14) 1 1.04(11)
O2 O 8 0.74159(40) 0.24565(42) 0.6248(14) 1 1.04(11)
O11 O 8 0.34296(32) 0.29910(39) 0.2213(15) 1 1.04(11)
O12 O 8 0.37685(52) 0.23623(38) 0.36955(86) 1 1.04(11)
C11 C 8 0.3840027 0.2652319 0.2677798 1 1.04(11)
C12 C 8 0.4441725 0.2638812 0.2012799 1 1.04(11)
C13 C 8 0.5006852 0.2601662 0.2677391 1 1.04(11)
C14 C 8 0.5577711 0.2687669 0.2051014 1 1.04(11)
C15 C 8 0.6164345 0.2752286 0.2755989 1 1.04(11)
C16 C 8 0.4452378 0.2729684 0.07067272 1 1.04(11)
C17 C 8 0.5020659 0.279699 0.00779776 1 1.04(11)
C18 C 8 0.5581572 0.277825 0.07447133 1 1.04(11)
O13 O 8 0.65747(27) 0.31092(38) 0.2350(10) 1 1.04(11)
O14 O 8 0.61520(41) 0.23827(41) 0.36435(83) 1 1.04(11)
O21 O 8 0.61510(55) 0.23349(31) 0.61487(83) 1 1.04(11)
O22 O 8 0.66472(30) 0.17040(42) 0.74989(87) 1 1.04(11)
C21 C 8 0.6168703 0.1874452 0.6826409 1 1.04(11)
C22 C 8 0.5579917 0.1683365 0.7451753 1 1.04(11)
C23 C 8 0.4992116 0.1899503 0.7029915 1 1.04(11)
C24 C 8 0.4436339 0.1675857 0.7585928 1 1.04(11)
C25 C 8 0.381207 0.1858979 0.710291 1 1.04(11)
C26 C 8 0.5605369 0.1251226 0.845279 1 1.04(11)
C27 C 8 0.5056948 0.103576 0.9015392 1 1.04(11)
C28 C 8 0.4476166 0.1243813 0.8585278 1 1.04(11)
O23 O 8 0.37952(50) 0.22270(41) 0.61569(86) 1 1.04(11)
O24 O 8 0.33152(34) 0.16816(47) 0.7590(13) 1 1.04(11)
Og1 O 8 0.15210(78) 0.16123(66) 0.3571(21) 1.000(23) 1.04(11)
Og2 O 8 0.05963(71) 0.07394(87) 0.3881(22) 0.759(19) 1.04(11)
Og3 O 8 -0.07003(67) 0.07315(78) 0.4043(17) 1.000(24) 1.04(11)
Og4 O 8 0.65907(81) 0.32458(79) 0.8033(18) 1.000(23) 1.04(11)
Og5 O 8 0.44584(79) 0.12564(78) 0.4407(20) 1.000(25) 1.04(11)
Og6 O 8 0.43204(58) -0.00025(55) 0.5665(14) 1.000(27) 1.04(11)
Og7 O 8 0.5 0 0.3511(57) 0.209(31) 1.04(11)

4) Modelling details of CAU-10-H

For the derivation of the partial charges of the CAU-10-H the Electronegativity Equalization Method (EEM) was employed following the approach described in a previous work². Three parameters were used for each atom as input to the EEM to compute the partial charges in CAU-10-H; electronegativity, hardness, and gamma factor (see Table S4). These parameters were taken from analogous parameters of the aluminum-based carboxylate MOF, the MIL-100(Al), since these two MOFs consist of similar atom types. These EEM parameters were calculated on a small cluster of MIL-100(Al) so as to obtain the same partial charges as the ones derived by Density Functional Theory computations on the same cluster³. The implementation of the EEM for the unit cells of CAU-10-H resulted in the mean values for the partial charges shown in Table S4.

The above partial charges were employed in a fully flexible model for CAU-10-H used in the Molecular Dynamics simulations. The initial parameters for bonded and dispersion interactions were taken from Dreiding⁴; then the following modifications were made in order to achieve the best possible matching with the IR spectrum of the crystal:

(i) The equilibrium bond distances, r_{ij}^0 , (Table S5) and angle values, θ_j^0 , (Table S6) were taken from the crystallographic data provided by the University of Kiel.

(ii) Except of the bond Al-O1 (that contributes to the stability of the chain of the cis-connected corner-sharing aluminium polyhedra), which was made stronger by shortening its equilibrium bond distance and increasing its force constant (see Table S5); it is worth mentioning that crystallography shows that this bond is slightly shorter than the rest Al-O bonds of the AlO_6 polyhedra.

(iii) The dispersion parameters for the bridging OH atoms (O1 and H7) were distinguished from the other oxygens and hydrogen atoms of CAU on the basis of their different electron charge (see Table S4); the charges on the O1 and H7 imply that the electrons of the hydrogen atom are shifted closer to the oxygen atom and, consequently the hydrogen atom is behaving like a point charge allowing for the proximity of other electronegative atoms (guest water oxygens) towards the creation of hydrogen bonding. To properly account for this, we used the dispersion parameters of the SPC/E model for the O1 and H7 which has been shown to describe well the formation of hydrogen bonds in liquid water⁵.

(iv) The torsional potential for the four dihedral angles (O2-C6-C5-C1, O2-C6-C5-C3, O3-C6-C5-C1, O3-C6-C5-C3) was zeroed (see Fig. S5 for notation); these angles control the rotation

of the carboxylate group relative to the aromatic ring. Zeroing them enabled the quasi free rotation of the linkers. The quasi free rotation of the linker has been showed to better capture the host dynamics in our previous work on ZIF-8⁶. To verify the validity of our choice regarding the particular mobility of the linkers, a stiff version was also tested by imposing torsional potentials on them as dictated by Dreiding (see Table S7). This latter stiff model version for the linkers did not satisfactorily reproduce the experimental IR spectrum, it did not capture the linker dynamics upon water adsorption (Fig. S7) with respect to the Second Harmonic Generation (SHG) microscopy experiments of this work, and did not predict the structural transition of CAU cell upon water adsorption (Fig. S8, bottom). So, one could conclude that a realistic representation for CAU-10-H linkers definitely opts for flexible states.

All remaining parameters were left the same as in the Dreiding force field. The final parameters are given in Tables S4-S8. The notation of the framework atoms is shown in Fig. S5.

The potential interaction energy was computed as a sum of bonded and non-bonded energy terms:

$$U = U_{bonded} + U_{nonbonded}$$

$$\text{where } U_{bonded} = U_{bonds} + U_{angles} + U_{torsions}$$

$$\text{and } U_{nonbonded} = U_{dispersion} + U_{electrostatic}$$

The form of these terms is given below.

$$\text{Bond stretch: } E_{IJ} = \frac{1}{2} k_{IJ} (r_{IJ} - r_{IJ}^0)^2, \text{ for atom } I \text{ bonded to atom } J$$

$$\text{Angle bend: } E_{IJK} = \frac{1}{2} k_{IJK} (\theta_{IJK} - \theta_j^0)^2, \text{ for two bonds } IJ \text{ and } JK$$

$$\text{Proper torsion: } E_{IJKL} = \frac{1}{2} V_{JK} \left\{ -\cos \left[n_{JK} (\varphi - \varphi_{JK}^0) \right] \right\}, \text{ for two bonds } IJ \text{ and } KL \text{ connected via a common bond } JK$$

$$\text{Improper torsion: } E_{IJKL} = K [1 - \cos \Psi], \Psi^0 = 0^\circ, \text{ for an atom } I \text{ bonded to exactly three other atoms, } J, K, L, \text{ and planar equilibrium geometry. The angle is between the } IL \text{ bond and } JIK \text{ plane.}$$

The dispersion interaction cutoff was 1.0 nm. The Lorentz–Berthelot rules were applied for describing guest–host interactions. Electrostatic interactions were computed through a particle-mesh Ewald summation code.

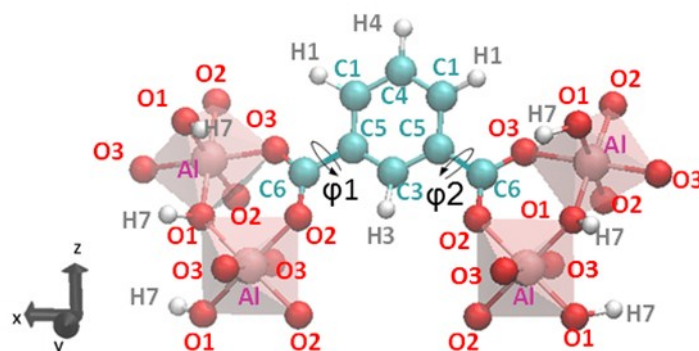


Fig. S5 CAU-10-H atom notation; definition of the dihedrals O2-C6-C5-C1 (φ_1 and φ_2) denoting the motion of the carboxylate group relative to the aromatic ring.

Table S4 Non-bonded and EEM parameters for the CAU-10-H atoms.

atom type	atom	ϵ (kcal/mol)	σ (Å)	EEM type	χ (eV/e)	2η (eV/e ²)	γ (Å ⁻³)	partial charge (e)
Al	Al	0.3100	3.9110	Al	0.8707	12.0000	0.5443	1.7116
O1	O	0.1554 ^a	3.1656 ^a	OH	11.380	16.6244	1.0898	-1.1303
O2	O	0.0957	3.0332	OT	7.2560	16.6244	1.0898	-0.5997
O3	O	0.0957	3.0332	OT	7.2560	16.6244	1.0898	-0.5883
C1	C	0.0951	3.4730	CAR2	5.7396	14.0000	0.9000	-0.1785
C3	C	0.0951	3.4730	CAR2	5.7396	14.0000	0.9000	-0.2173
C4	C	0.0951	3.4730	CAR2	5.7396	14.0000	0.9000	-0.0993
C5	C	0.0951	3.4730	CAR	4.9896	14.0000	0.9000	-0.0237
C6	C	0.0951	3.4730	CT	3.7426	14.0000	0.9000	0.7103
H1	H	0.0152	2.8464	HAR	3.0656	20.1678	0.8910	0.1820
H3	H	0.0152	2.8464	HAR	3.0656	20.1678	0.8910	0.2157
H4	H	0.0152	2.8464	HAR	3.0656	20.1678	0.8910	0.1580
H7	H	0.0000 ^a	--- ^a	HOH	4.3178	19.2186	0.8203	0.3574

^a SPC/E parameters for the O1 and H7 atoms of the bridging OH group

Table S5 Bond stretch parameters for the CAU-10-H.

<i>I-J</i>	k_{IJ} (kcal/mol/ \AA^2)	r_{IJ}^0 (\AA)
C1-C4	1050	1.39
C1-C5	1050	1.39
C3-C5	1050	1.39
C1-H1	700	1.02
C3-H3	700	1.02
C4-H4	700	1.02
C5-C6	700	1.47
Al-O1	2800	1.70
Al-O2	700	1.90
Al-O3	700	1.89
O1-H7	700	1.00
O2-C6	700	1.25
O3-C6	700	1.28

Table S6 Angle bend parameters for the CAU-10-H.

<i>I-J-K</i>	k_{IJK} (kcal/mol/rad ²)	θ_J^0 (degrees)
C1-C4-C1	100	120
C4-C1-C5	100	120
C1-C5-C3	100	120
C5-C3-C5	100	120
C3-C5-C1	100	120
C5-C1-C4	100	120
C1-C4-H4	100	120
C1-C4-H4	100	120
C4-C1-H1	100	120
C5-C1-H1	100	120

C1-C5-C6	100	120
C3-C5-C6	100	120
C5-C3-H3	100	120
C5-C3-H3	100	120
C3-C5-C6	100	120
C1-C5-C6	100	120
C5-C1-H1	100	120
C4-C1-H1	100	120
O1-AI-O1	100	90
O2-AI-O2	100	90
O3-AI-O3	100	180
O1-AI-O2	100	180
O1-AI-O2	100	90
O1-AI-O3	100	90
O2-AI-O3	100	90
AI-O2-C6	100	130.4
AI-O3-C6	100	136.6
O2-C6-C5	100	117.1
O3-C6-C5	100	117.1
O2-C6-O3	100	120
AI-O1-AI	100	126.6

Table S7 Torsion interaction parameters for the CAU-10-H.

<i>I-J-K-L</i>	V_{JK} (kcal/mol)	n_{JK}	φ_{JK}^0 (degrees)
C4-C1-C5-C3	25	2	0
C1-C5-C3-C5	25	2	0
C5-C3-C5-C1	25	2	0
C3-C5-C1-C4	25	2	0
C5-C1-C4-C1	25	2	0
C1-C4-C1-C5	25	2	0
C4-C1-C5-C6	25	2	0
C1-C5-C3-H3	25	2	0
C5-C3-C5-C6	25	2	0
C3-C5-C1-H1	25	2	0
C5-C1-C4-H4	25	2	0
C1-C4-C1-H1	25	2	0
C5-C1-C4-H4	25	2	0
C1-C4-C1-H1	25	2	0
C4-C1-C5-C6	25	2	0
C1-C5-C3-H3	25	2	0
C5-C3-C5-C6	25	2	0
C3-C5-C1-H1	25	2	0
H4-C4-C1-H1	25	2	0
H1-C1-C4-H4	25	2	0
H1-C1-C5-C6	25	2	0
H3-C3-C5-C6	25	2	0
H3-C3-C5-C6	25	2	0
H1-C1-C5-C6	25	2	0
O2-C6-C5-C1	5	2	0
O2-C6-C5-C3	5	2	0
O3-C6-C5-C1	5	2	0
O3-C6-C5-C3	5	2	0

Table S8 Improper torsion interaction parameters for CAU-10-H.

<i>I-J-K-L</i> (central <i>I</i>)	K (kcal/mol/rad ²)
C4-C1-C1-H4	40
C1-C5-C4-H1	40
C5-C3-C1-C6	40
C3-C5-C5-H3	40
C5-C1-C3-C6	40
C1-C4-C5-H1	40
C6-O2-O3-C5	40

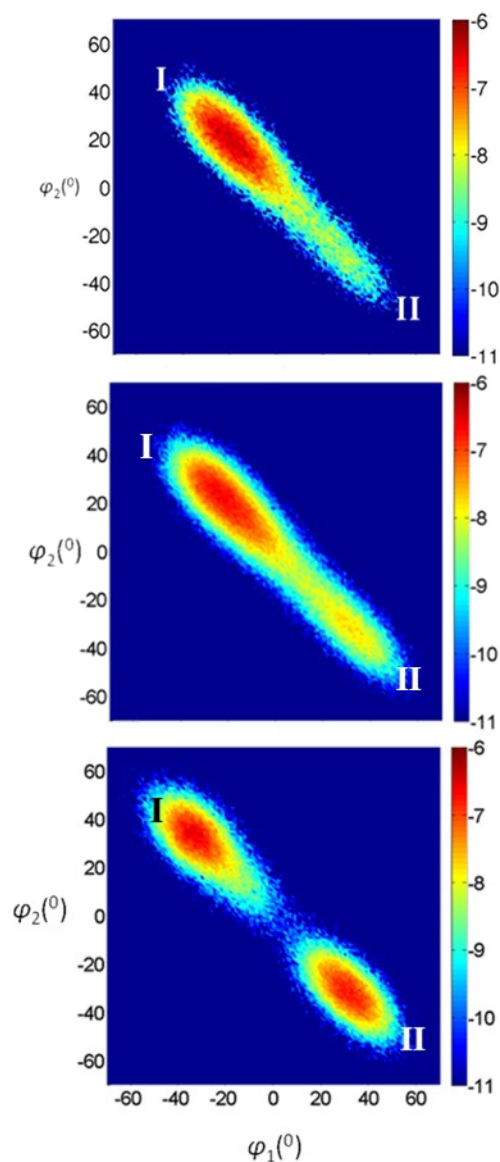


Fig. S6 Correlation probabilities calculated by MD of the dihedral angles φ_1 and φ_2 for the CAU-10-H linkers, for the model option enabling quasi-free rotation of the linkers, for the dehydrated (top), and the water-loaded CAU-10-H at loadings of 0.032 (middle) and 0.303 gg^{-1} (bottom). Colour code: low (blue) to high (red) probability values (in natural logarithmic scale). See analogous figure in the article, illustrating only the dehydrated (top) and the loading of 0.303 gg^{-1} (bottom).

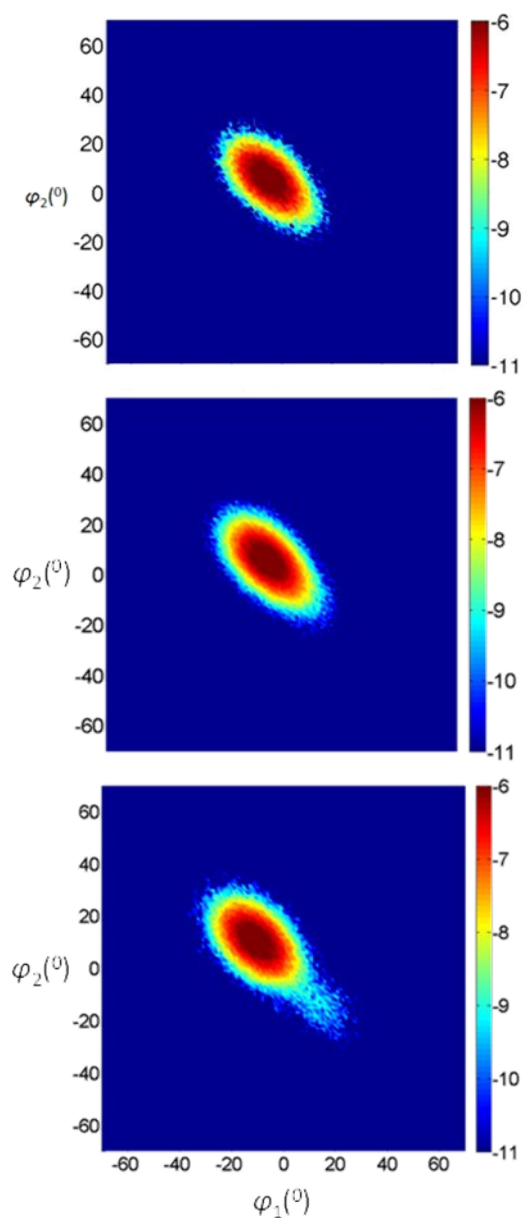


Fig. S7 Correlation probabilities calculated by MD for the dihedral angles φ_1 and φ_2 , for the model option imposing torsional potentials on the linkers, for the dehydrated (top), and the water-loaded CAU-10-H at loadings of 0.032 (middle) and 0.303 gg^{-1} (bottom). Colour code: low (blue) to high (red) probability values (in natural logarithmic scale).

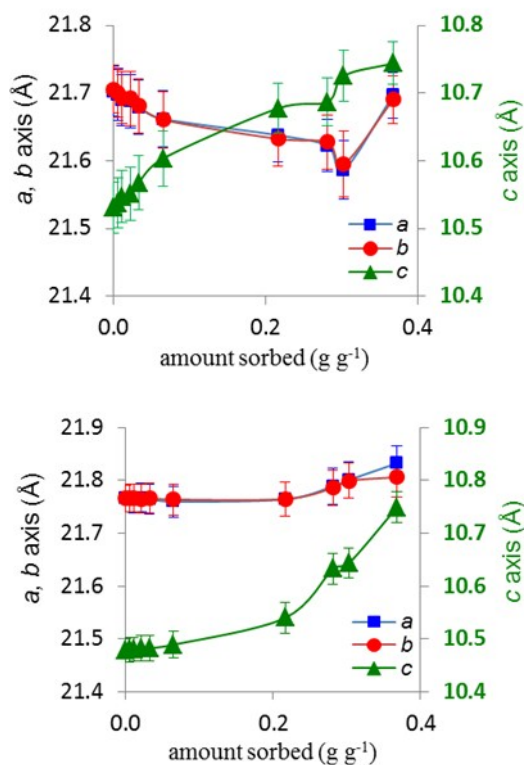


Fig. S8 Simulated length evolution of the *a*, *b* and *c* axes of the CAU-10-H crystal unit cell induced by the water adsorption during an MD trajectory, as a function of loading: 0.005, 0.011, 0.022, 0.032, 0.065, 0.216, 0.281, 0.303 and 0.368 g g⁻¹, using the Andersen conventional isobaric algorithm in MD simulations, for the two model options: enabling quasi-free rotation of the linkers (top) and imposing torsional potentials on them (bottom).

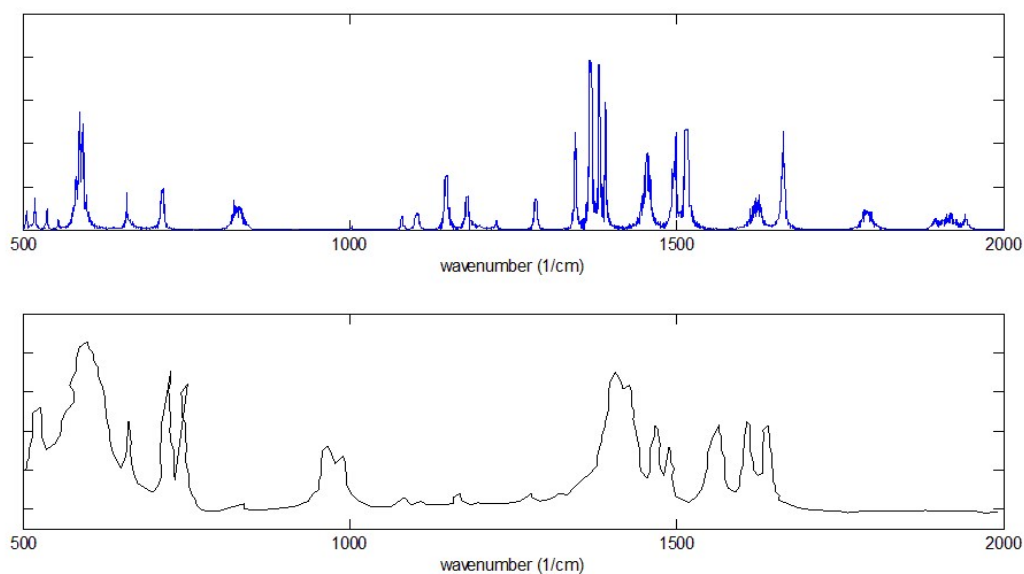


Fig. S9 Computed (top) and measured¹ (bottom) IR spectra of CAU-10-H.

We note that we have not simulated an identical IR spectrum with the measured one as this is extremely difficult and practically impossible although we tried hard because of the many degrees of freedom of the mobile CAU system of atoms. For this reason we also added error bars to all modelling experiments (Fig. 10 and Fig. 12 in paper). Also the spectrum is what we found from the last stage Fourier post-MD-processing namely raw results with no smoothing or fitting job on them. The alternative route of deriving ad hoc quantum mechanical parameters and then fitting for CAU-10-H is completely out of scope of this work because we cannot perform ab initio calculations of this type. Concluding we tried to make a reasonable adjustment of parameters, however; so that our modelling results will be reproducible.

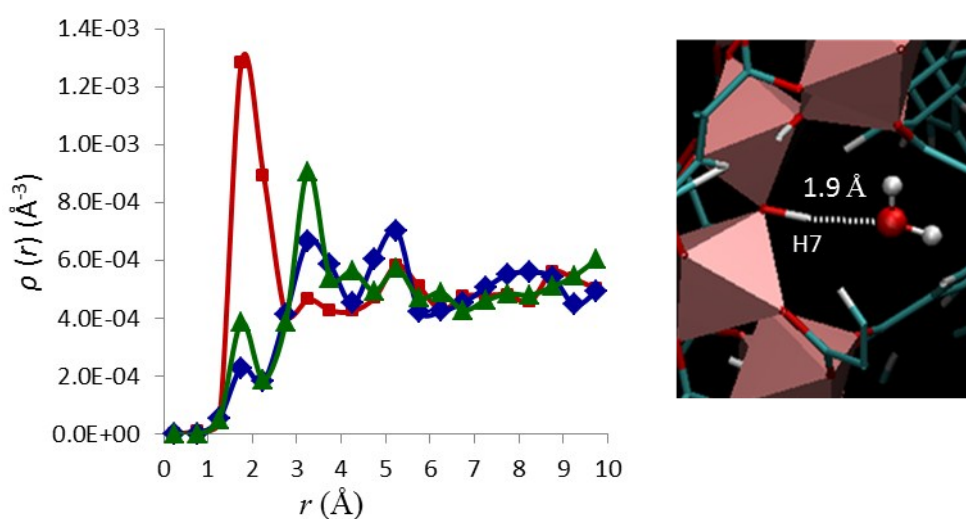


Fig. S10 Density distribution functions of the guest water oxygens calculated with respect to the hydrogen atom (H7) of the bridging OH group (squares) and the O2 (rhombi) and O3 (triangles) oxygens of the carboxylate groups (see Fig. S5 for atoms notation) at low loading 0.011 gg^{-1} ; on the right is depicted a snapshot from MD simulations showing the distance between the H7 atom of the bridging OH group and a guest water molecule.

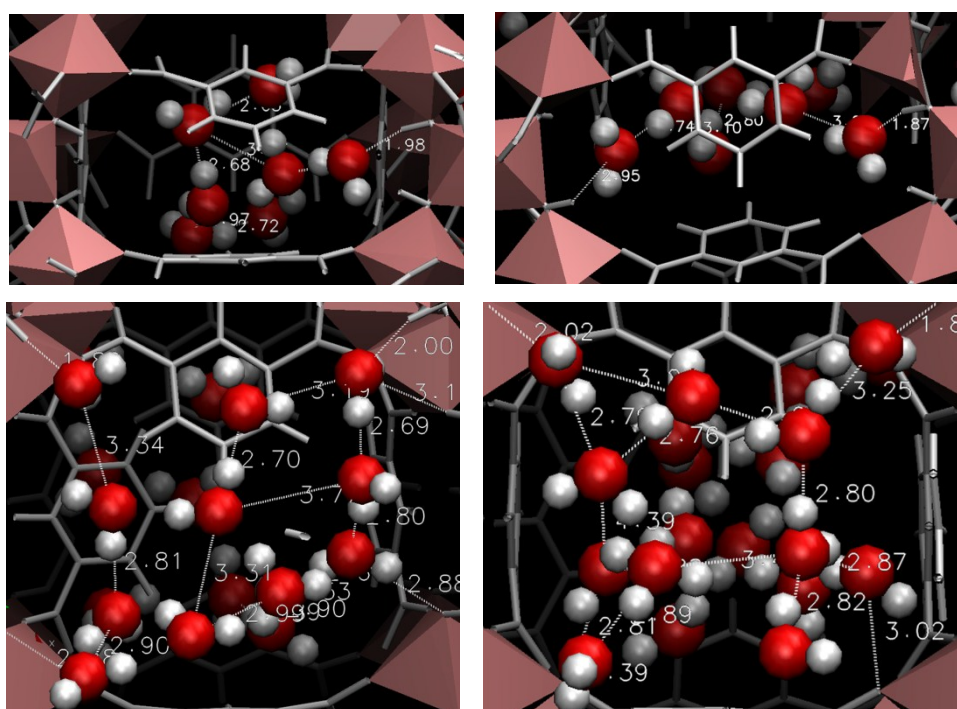


Fig. S11 Indicative snapshots from MD simulation depicting the formation of water clusters at 0.065 (top, middle) and 0.216 gg^{-1} loadings (bottom); colour code: aluminium polyhedra (pink), water molecule (H: white and O: red), linker and bridging OH group (grey).

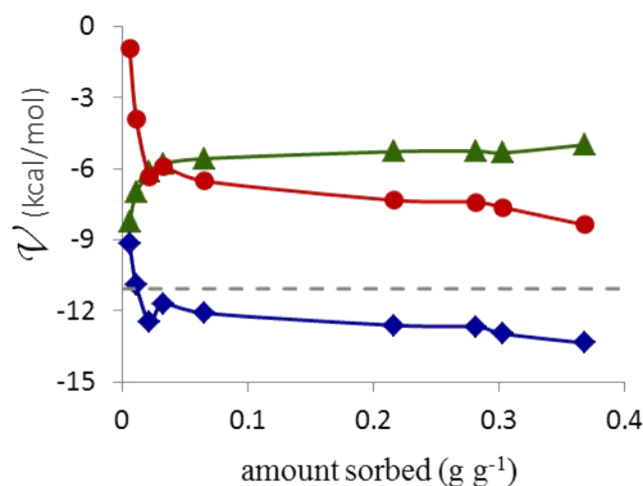


Fig. S12 Guest–guest (circles) and guest–host (triangles) components of the total potential energy (rhombi) in the water/CAU-10-H system at 300 K as a function of loading; the dashed line points to the energy of liquid water at 300 K computed via the SPC/E model.

References

1. H. Reinsch, M. A. van der Veen, B. Gil, B. Marszalek, T. Verbiest, D. de Vos and N. Stock, *Chem. Mater.*, 2013, **25**, 17.
2. P. D. Kolokathis, E. Pantatosaki and G. K. Papadopoulos, *J. Phys. Chem. C*, 2015, **119**, 20074-20084.
3. Details provided in forthcoming publication by Pantatosaki et al.
4. S. L. Mayo, B. D. Olafson and W. A. Goddard, *J. Phys. Chem.*, 1990, **94**, 8897.
5. J. M. Sorenson, G. Hura, R. M. Glaeser and T. Head-Gordon, *J. Chem. Phys.* **2000**, **113**, 9149-9161.
6. E. Pantatosaki, G. Megariotis, A.-K. Pusch, C. Chmelik, F. Stallmach and G. K. Papadopoulos, *J. Phys. Chem. C*, **2012**, **116**, 201–207.